Pergamon

Int. J. Heat Mass Transfer. Vol. 39, No. 2, pp. 235–246, 1996

0017-9310/96 $9.50+0.00

0017-9310(95)00127-1

Homogeneous nucleation of vapor by depressurization at constant volume

C. D. SULFREDGE, K. A. TAGAVI and L. C. CHOW†
Department of Mechanical Engineering, University of Kentucky, Lexington, KY 40506, U.S.A.

(*Received* 28 *October* 1994 *and in final form* 16 *March* 1995)

Abstract—An analysis has been carried out to determine the thermodynamic requirements for homogeneous nucleation of a vapor bubble when the pressure drops inside a constant-volume container of liquid. This situation can occur in phase change processes when a rigid vessel filled with liquid is cooled. The nucleation equations at constant volume have a somewhat different character from their more familiar constant-pressure counterparts that reflects the change in the boundary conditions for bubble formation. Both the physical and mathematical implications of the new solution are explored in detail, and it is shown to reduce to the well known constant-pressure result in the limiting case of a very large container volume. To illustrate an application of the new equations, some numerical examples have been worked out for homogeneous nucleation of water with various container sizes and initial liquid temperatures. In addition to increasing fundamental understanding of homogeneous nucleation, these results should prove valuable for calculation purposes when vapor nucleation takes place under isochoric rather than isobaric conditions.

INTRODUCTION

By taking advantage of the latent heat of a phase change material (PCM), one can absorb or give off a great deal of thermal energy while the system temperature remains almost constant. However a change of phase is always accompanied by a change in density as the molecules rearrange into their new atomic structure. The solid phase of almost all PCM's has a more closely spaced atomic arrangement than the corresponding liquid phase, and hence a higher density. It follows that shrinkage voids must be created in the PCM when solidification takes place under the constant-volume conditions typical of many thermal energy storage (TES) systems. Because the shrinkage void distribution is of vital importance when one attempts to remelt the frozen PCM, several papers by the present authors [1–3] have analyzed these voids for various TES configurations and rates of freezing. Initial appearance of shrinkage voids during solidification of a phase change material requires nucleation of vapor-filled bubbles in the liquid phase. One question left unanswered by our previous analyses concerns the relative importance of homogeneous and heterogeneous nucleation in this bubble-formation process.

Regardless of the nucleation mode, the main resistance to nucleation of a vapor bubble is due to an energy barrier arising from capillary forces and the surface tension of the liquid phase. The fundamental capillary relationship for the pressure difference across the liquid–vapor interface during bubble nucleation is known as Laplace's equation [4]. If the bubble is assumed to be spherical with radius r, then the resulting criterion for mechanical equilibrium is

$$P_v - P_l = 2\sigma/r \tag{1}$$

where σ is the liquid surface tension. Laplace's relation clearly shows that a higher pressure on the concave or vapor side of the interface is necessary for mechanical equilibrium of a bubble. Simultaneously, the bubble must have $T_v = T_l$ in order to satisfy the requirements of thermal equilibrium. Combining this result with equation (1) and noting that $T_v = T_{sat}(P_v)$, it follows that

$$T_l = T_{sat}(P_v) = T_{sat}(P_l + 2\sigma/r) > T_{sat}(P_l). \tag{2}$$

Hence the surrounding liquid must be superheated relative to the prevailing pressure in order to overcome the surface tension energy barrier so that thermomechanical equilibrium is satisfied and nucleation of a vapor bubble can occur. Both homogeneous nucleation and heterogeneous nucleation are possible mechanisms for overcoming the energy barrier to initiate vapor formation in the liquid phase. While most practical boiling applications involve heterogeneous nucleation, homogeneous nucleation is very important from a theoretical standpoint and in the limiting case of a very pure liquid with no cavities available to seed heterogeneous bubbles.

Although Laplace's equation dates back to 1805, the influence of surface free energy on nucleation remained uninvestigated for some time. One of the earliest analyses of this type concerned the initial formation of solid during freezing of a liquid, when Turnbull [5] and Holloman and Turnbull [6] calculated the conditions for homogeneous nucleation of the solid phase in metal casting. Slightly more com-

† Author to whom correspondence should be addressed.

NOMENCLATURE

A	availability
F	Helmholtz free energy
f	specific Helmholtz free energy
g	specific Gibbs free energy
h_p	Planck's constant
J	homogeneous nucleation frequency, [nucleations $m^{-3} s^{-1}$]
k	Boltzmann's constant
M	molecular weight
n	number of molecules
N_{av}	Avogadro's number
P	absolute pressure
r	bubble radius
S	entropy
s	specific entropy
T	absolute temperature
U	internal energy
u	specific internal energy
V	volume
v	specific volume.

Greek symbols

ζ	ratio of container volume to critical bubble volume, $V/((4/3)\pi r_c^3)$
κ_t	isothermal compressibility factor
μ	chemical potential
ρ	mass density
σ	surface tension
τ	unit time used to express the molecular collision frequency.

Subscripts

c	critical radius
comp	effect due to liquid compression
infl	inflection condition of the potential curve
l	liquid phase
max	maximum bubble growth size
o	initial conditions
P	constant pressure conditions
sat	saturation conditions
sp	spinodal line conditions
t	total number of molecules
tot	total pressure drop
V	constant volume conditions
v	vapor phase.

plicated versions of their equations are also applicable to formation of vapor bubbles in a liquid under constant pressure conditions [7, 8]. As a result, the constant-pressure homogeneous nucleation case is relatively well understood. Unfortunately, these results are not directly applicable to the problem of bubble formation under the constant-volume depressurization conditions encountered when freezing a liquid PCM. This article will use the constant-pressure analysis for homogeneous nucleation of vapor bubbles reported by Carey [9] as a starting point to develop a model valid under constant volume conditions.

HOMOGENEOUS NUCLEATION AT CONSTANT PRESSURE

Carey's calculations [9] began with a collection of n_t molecules of which n_v form a spherical embryo in an activated (vapor) state. The free surface of the liquid is assumed to be subjected to some constant pressure P_l. Thus the thermodynamic availability function at constant pressure will be defined as $A_P = U - T_l S + P_l V$, the maximum amount of work that could be reversibly extracted by bringing the system to the dead state at T_l and P_l. The total availability of all the molecules is then composed of three terms: the availability contribution of the vapor bubble, that of the surrounding liquid, and the free energy of the bubble interface. Hence one has

$$A_P = A_v + A_l + A_{interface}. \tag{3}$$

Now the individual availability terms can be expressed by

$$\begin{aligned} A_l &= n_l(u_l - T_l s_l + P_l v_l) \\ &= (n_t - n_v) g_l(T_l, P_l) \\ A_v &= n_v(u_v - T_l s_v + P_l v_v) \\ &= n_v[g_v(T_l, P_v) + (P_l - P_v)v_v] \\ A_{interface} &= 4\pi r^2 \sigma \end{aligned} \tag{4}$$

where g_l is the specific Gibbs free energy of each liquid molecule and g_v represents the same function for a vapor molecule. Gibbs free energy is the relevant thermodynamic potential governing the equilibrium state because the nucleation process will take place at constant temperature and external pressure.

Substituting these expressions back into equation (3) and defining the excess availability at constant pressure, ΔA_P, by $\Delta A_P = A_P - n_t g_l(T_l, P_l)$ gives:

$$\Delta A_P = n_v[g_v(T_l, P_v) - g_l(T_l, P_l) + (P_l - P_v)v_v] + 4\pi r^2 \sigma. \tag{5}$$

One should note from equation (5) that the Gibbs potential of the overall liquid–vapor system differs from the result one would obtain by simply summing the Gibbs potentials of the component subsystems because of the pressure difference across the liquid–

vapor interface [10]. Failure to account for this fact would cause the $(P_l - P_v)v_v$ term to be missing from equation (5). Now the number of vapor molecules, n_v, can be related to the embryo radius by $n_v = \frac{4}{3}\pi r^3 \rho_v (N_{av}/M)$ where N_{av} is Avogadro's number and M is the molecular weight.

$$\Delta A_P = \tfrac{4}{3}\pi r^3 \rho_v \frac{N_{av}}{M}[g_v(T_l, P_v) - g_l(T_l, P_l) + (P_l - P_v)v_v] + 4\pi r^2 \sigma. \quad (6)$$

For a pure substance, the specific Gibbs free energy is equivalent to the chemical potential so $g_l = \mu_l$ and $g_v = \mu_v$. Furthermore μ_l must equal μ_v for mass diffusion equilibrium between the vapor bubble and the surrounding liquid. Thus at $r = r_c$, the critical bubble radius for homogeneous nucleation, $(P_l - P_v)v_v = -2\sigma/r_c$ by Laplace's equation while g_v and g_l cancel one another, leaving $\Delta A_P(r = r_c) = \frac{4}{3}\pi r_c^2 \sigma$ [9]. If one substitutes the Taylor-series approximation $g_v(T_l, P_v) \approx g_v(T_l, P_l) + v_v(P_v - P_l)$ into equation (6), it is possible to develop a very simple expression for ΔA_P as a function of bubble radius. The value just derived for $\Delta A_P(r = r_c)$ then implies $g_v(T_l, P_l) - g_l(T_l, P_l) = -2\sigma M v_v / r_c N_{av}$ so that the approximate potential curve will have the correct magnitude at $r = r_c$. Equation (6) thus reduces to the important result

$$\Delta A_P = 4\pi r^2 \sigma \left[1 - \frac{2}{3}\frac{r}{r_c}\right] \quad (7)$$

which Cole [11] derived under a slightly different set of assumptions. The excess availability, ΔA_P, is sketched vs r in Fig. 1. Clearly $r = r_c$ corresponds to a local maximum of the curve. For $r < r_c$, the bubble tends to shrink until it disappears since shrinkage will always be accompanied by decreasing availability. Once r exceeds r_c, further enlargement is always associated with decreasing ΔA_P, and continued bubble growth will be favored.

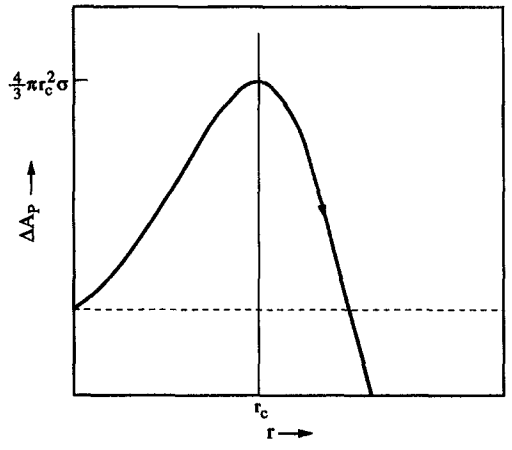

Fig. 1. Sketch of the excess availability vs bubble radius at constant pressure.

HOMOGENEOUS NUCLEATION AT CONSTANT VOLUME

Equation (7) gives the fundamental availability potential of the liquid–vapor system as a function of bubble radius under constant pressure conditions. However it does not represent all the physics involved in homogeneous bubble formation inside a rigid container completely filled with liquid. This is the isochoric situation at the onset of nucleation when cooling the phase change material in TES systems prior to actual solidification. Solidification shrinkage itself has no effect on the depressurization requirements for nucleation and only influences bubble growth after nucleation takes place. The following analysis will examine the problem of homogeneous nucleation at constant volume from first principles and point out several important physical differences between isobaric and isochoric homogeneous nucleation.

As a first step, consider the situation in which a container of constant volume V encloses a total of n_t molecules at temperature T_l. Of these n_t molecules, n_v are assumed to be in an activated or vapor state, forming a spherical nucleus of radius r. Because the system is now subjected to conditions of uniform temperature and constant overall volume, the thermodynamic availability function must be redefined as $A_V = U - T_l S$, the maximum work that can be extracted in a constant-volume transition at the dead state temperature T_l. Including the interfacial availability term, the total availability of all the molecules in the container will then be given by the equation

$$A_V = (n_t - n_v)f_l(T_l, v_l') + n_v f_v(T_l, v_v) + 4\pi r^2 \sigma. \quad (8)$$

In this equation, f_l is the Helmholtz free energy of the liquid phase, f_v is the Helmholtz free energy of the vapor phase, n_t is the total number of molecules, and n_v is the number of vapor molecules. Here v_l' stands for the liquid specific volume after compression by the nucleated bubble, and v_l will later be used to represent the liquid's specific volume before any bubble was present.

Specifying a constant volume condition instead of constant pressure has caused the Helmholtz function to replace the Gibbs function as the relevant thermodynamic potential, in contrast to conventional homogeneous boiling theory. In addition, equation (8) shows that the Helmholtz potential of the total liquid–vapor system does indeed equal the sum of the Helmholtz potentials for its constituent subsystems. Unlike the Gibbs potential appearing in the constant-pressure case described by equation (5), the pressure difference across the bubble interface has no effect on the respective Helmholtz functions. Equality of temperature for the two phases is all that is necessary for the sum of the subsystem Helmholtz potentials to be applicable when analyzing the overall system.

For an analysis at constant volume, it is necessary to define the constant-volume excess availability in terms of $\Delta A_V = A_V - n_t f_l(T_l, v_l)$. Putting equation (8) into this form yields:

$$\Delta A_V = n_v[f_v(T_l, v_v) - f_l(T_l, v_l')] + n_t[f_l(T_l, v_l') - f_l(T_l, v_l)] + 4\pi r^2\sigma. \quad (9)$$

Adding and subtracting $n_v f_l(T_l, v_l)$ and rearranging, then relating n_v to the radius of the embryo bubble and the vapor density as was done for the constant-pressure case, shows that

$$\Delta A_V = (4/3)\pi r^3 \rho_v \frac{N_{av}}{M}[f_v(T_l, v_v) - f_l(T_l, v_l)] + 4\pi r^2\sigma + (n_t - n_v)[f_l(T_l, v_l') - f_l(T_l, v_l)]. \quad (10)$$

The first term in equation (10) represents the availability change resulting from vaporizing the n_v liquid molecules, the $4\pi r^2\sigma$ group is the free energy of the liquid–vapor interface, and the third term stands for the change in availability of the remaining liquid molecules due to compression of the liquid in the constant-volume container.

The next step is to find an expression for the liquid compression term $(n_t - n_v)[f_l(T_l, v_l') - f_l(T_l, v_l)]$, which from this point on will be denoted by ΔF_{comp}. Thus one has

$$\Delta F_{comp} = \Delta U_l - T_l \Delta S_l = -\int_{V-\varepsilon}^{V_l'} P_l \, dV_l \quad (11)$$

so that ΔF_{comp} can be related to the work done by the bubble in compressing the liquid. In equation (11), ε is the volume originally occupied by the liquid molecules that were later vaporized, and V_l' is the liquid volume after nucleation. If one considers ε to be negligibly small relative to the eventual bubble volume, then $V_l = V - (4/3)\pi r^3$ and it follows that

$$\Delta F_{comp} = \int_0^r P_l(r) 4\pi r^2 \, dr \quad (12)$$

when the integrand is transformed in terms of r instead of V_l. From the definition of the isothermal compressibility of a liquid, κ_t, one obtains [12]:

$$\kappa_t = -(1/v_l)\left.\frac{\partial v_l}{\partial P_l}\right|_T \quad \text{or} \quad \left.\frac{\partial P_l}{\partial v_l}\right|_T = -1/(\kappa_t v_l) \quad (13)$$

where v_l is the molar specific volume.

Now this expression can be solved as a differential equation for P_l as a function of v_l, assuming κ_t is essentially constant over the specific volume range of interest. The solution can then be converted to yield $P_l(r)$ if one notes that

$$v_l = \frac{V - V_{bubble}}{n_t - n_v} = \frac{V - (4/3)\pi r^3}{n_t - (4/3)\pi r^3\left(\rho_v \frac{N_{av}}{M}\right)} \quad (14)$$

where ρ_v is the vapor density. Integrating the differential equation at constant T_l gives

$$P_l(r) = P_o + \frac{1}{\kappa_t}\ln\left\{\frac{[n_t - (4/3)\pi r^3 \rho_v N_{av}/M]/n_t}{[V - (4/3)\pi r^3]/V}\right\} \quad (15)$$

in which P_o is the liquid pressure prior to any nucleation. This equation for $P_l(r)$ must now be substituted into the integral to evaluate ΔF_{comp}. Carrying out the calculations yields

$$\Delta F_{comp} = \frac{Mn_t}{\kappa_t \rho_v N_{av}}\left(\frac{4\pi r^3 \rho_v N_{av}}{3Mn_t} - 1\right)\ln\left(1 - \frac{4\pi r^3 \rho_v N_{av}}{3Mn_t}\right) - \frac{V}{\kappa_t}\left(\frac{4\pi r^3}{3V} - 1\right)\ln\left(1 - \frac{4\pi r^3}{3V}\right) + \tfrac{4}{3}\pi r^3 P_o. \quad (16)$$

The result just obtained for ΔF_{comp} can now be put back into the expression for ΔA_V from equation (10) to obtain:

$$\Delta A_V = (4/3)\pi r^3 \rho_v \frac{N_{av}}{M}[f_v(T_l, v_v) - f_l(T_l, v_l)] + 4\pi r^2\sigma + \frac{Mn_t}{\kappa_t \rho_v N_{av}}\left(\frac{4\pi r^3 \rho_v N_{av}}{3Mn_t} - 1\right)\ln\left(1 - \frac{4\pi r^3 \rho_v N_{av}}{3Mn_t}\right) - \frac{V}{\kappa_t}\left(\frac{4\pi r^3}{3V} - 1\right)\ln\left(1 - \frac{4\pi r^3}{3V}\right) + \tfrac{4}{3}\pi r^3 P_o. \quad (17)$$

Just as in homogeneous nucleation at constant pressure, the system seeks to minimize ΔA_V by getting over the local maximum in excess availability at $r = r_c$. Thus one needs to set $\partial/\partial r(\Delta A_V) = 0$ in order to locate the critical radius corresponding to the peak of the availability curve. Solving the resulting equation for the Helmholtz free energy difference in terms of r_c and using it to eliminate $f_v(T_l, v_v) - f_l(T_l, v_l)$ from the expression for ΔA_V in equation (17), one has

$$\Delta A_V = (4/3)\pi\frac{r^3}{r_c^2}\left\{-2r_c\sigma - r_c^2 P_o - r_c^2/\kappa_t \times \ln\left[\frac{1 - 4\pi r_c^3 \rho_v N_{av}/3Mn_t}{1 - 4\pi r_c^3/3V}\right]\right\} + 4\pi r^2\sigma + \tfrac{4}{3}\pi r^3 P_o + \frac{Mn_t}{\kappa_t \rho_v N_{av}} \times \left(\frac{4\pi r^3 \rho_v N_{av}}{3Mn_t} - 1\right)\ln\left(1 - \frac{4\pi r^3 \rho_v N_{av}}{3Mn_t}\right) - \frac{V}{\kappa_t}\left(\frac{4\pi r^3}{3V} - 1\right)\ln\left(1 - \frac{4\pi r^3}{3V}\right). \quad (18)$$

Equation (18) defines the availability potential for constant-volume homogeneous nucleation as a function of bubble radius in a manner precisely analogous to the constant-pressure result in equation (7).

In order to complete either solution, one must introduce an expression for the rate at which thermal fluc-

tuations in the liquid phase form embryo bubbles with $r > r_c$. From the Boltzmann distribution of molecular energies [7], the homogeneous nucleation frequency J per unit volume can be related to the excess availability at the critical radius by

$$J = \frac{n_t k T_l}{h_p V} \exp\left\{\frac{-\Delta A(r_c)}{k T_l}\right\} \tag{19}$$

whether the boundary conditions for nucleation are constant pressure or constant volume. The symbol k included in equation (19) stands for Boltzmann's constant while h_p indicates Planck's constant.

For the already-familiar constant pressure solution, substituting equation (7) for $\Delta A_P(r)$ with $r = r_c$ into equation (19) and simplifying algebraically yields

$$r_c = \left\{\frac{3kT_l}{4\pi\sigma} \ln\left[\frac{n_t k T_l}{J h_p V}\right]\right\}^{1/2} \tag{20}$$

which allows the critical radius for homogeneous nucleation to be calculated once the liquid properties and nucleation frequency are available. Selection of the frequency, J, for homogeneous nucleation at constant pressure is somewhat subjective, depending on the level of nucleation one requires before considering the liquid to be 'boiling'. Experience seems to indicate that values of J between 10^9 and 10^{13} nucleations m^{-3} s^{-1} correspond to relatively vigorous homogeneous boiling [7].

The new constant-volume analysis leads to a rather more complicated expression for r_c when $\Delta A_V(r)$ from equation (18) with $r = r_c$ is inserted into equation (19):

$$J = [n_t k T_l / h_p V] \exp\left\{\frac{-1}{k T_l}\left[(4/3)\pi r_c^2 \sigma - \frac{M n_t}{\kappa_t \rho_v N_{av}} \ln\left(1 - \frac{4\pi r_c^3 \rho_v N_{av}}{3 M n_t}\right) + \frac{V}{\kappa_t} \ln\left(1 - \frac{4\pi r_c^3}{3V}\right)\right]\right\} \tag{21}$$

and it is no longer possible to solve for r_c in closed form. However some aspects of the selection of J under constant-volume conditions are a little more clear cut than in the constant-pressure solution developed previously. To have homogeneous nucleation, at least one bubble must be formed within the available volume of liquid by crossing the peak of the availability curve. Furthermore, imposition of a constant-volume boundary condition makes nucleation of more than one bubble inside the container unlikely. Previous work [2] has shown that "pressure communication", or equalization of pressure between liquid shrinkage bubbles during freezing of a liquid PCM, favors creation of a single shrinkage void to minimize the interfacial free energy associated with a given void volume. Once the first bubble has been formed according to homogeneous nucleation theory, pressure communication effects will strongly oppose any further nucleation, especially for container sizes small enough that the constant-volume restriction causes significant liquid compression. Forming more than one bubble would also imply a higher J and more deviation from equilibrium conditions, so a nucleation equation based on a single bubble in the container provides the minimum requirements for homogeneous nucleation. Therefore one would expect the correct J value at constant volume to be directly proportional to $(1/V)$ for any container volume V.

A time factor τ which reflects how long after depressurization nucleation takes place must also be selected in order to establish the homogeneous nucleation frequency J. It then follows that

$$J = \frac{1}{V \cdot \tau} \quad \text{(for constant-volume nucleation).} \tag{22}$$

Whatever τ is chosen needs to be reasonably long relative to the time scale of the depressurization process and the pressure communication time for the container dimensions involved. Like the overall J factor in constant-pressure homogeneous boiling, the choice of τ is rather subjective. Fortunately, changing τ has no effect on the behavior of r_c as a function of either the liquid temperature or the container volume. The functional dependence of the solution on τ is also rather weak, so that the calculated critical radius does not vary much even when τ is changed by many orders of magnitude. The selection of a specific value for τ will be addressed when some numerical examples are considered later in this paper.

From the preceding discussion, equation (22) should yield the minimum nucleation frequency necessary to place at least one vapor bubble inside the container during the characteristic time selected. Hence substituting the J value from equation (22) back into equation (21) allows one to solve for the minimum departure from thermodynamic equilibrium required to initiate homogeneous nucleation under constant-volume conditions. The resulting expression will be in a somewhat more convenient form if one also notes that $V = n_t M / N_{av} \rho_l$ and rearranges the equation to give

$$k T_l \ln\left(\frac{N_{av} \rho_l k T_l V \tau}{M h_p}\right) = \tfrac{4}{3}\pi r_c^2 \sigma - \frac{V(\rho_l/\rho_v)}{\kappa_t} \times \ln\left(1 - \frac{4\pi r_c^3 (\rho_v/\rho_l)}{3V}\right) + \frac{V}{\kappa_t} \ln\left(1 - \frac{4\pi r_c^3}{3V}\right) \tag{23}$$

which is the desired constant-volume counterpart of the well known constant-pressure solution from equation (20). The next section will investigate many of the properties of this new result and show how its predictions relate to the physics of homogeneous nucleation under isochoric boundary conditions.

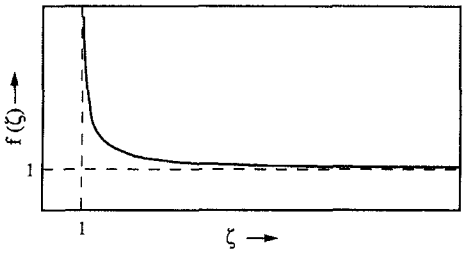

Fig. 2. Sketch showing the behavior of the function $f(\zeta)$.

ANALYSIS AND DISCUSSION

Characteristics of the isochoric potential curve

Work with the new isochoric solution from equation (23) should begin by developing a qualitative understanding of the behavior of the logarithmic liquid compressibility terms that now appear in the equation. In order to illustrate the effect of these terms better, it is helpful to define a new variable $\zeta = V/\frac{4}{3}\pi r_c^3$ which combines both V and r_c in dimensionless form, then rewrite equation (23) as

$$kT_l \ln\left(\frac{N_{av}\rho_l kT_l V\tau}{Mh_p}\right) = \tfrac{4}{3}\pi r_c^2\left[\sigma - \frac{r_c}{\kappa_t}\left(f(\zeta) - f\left(\frac{\rho_l}{\rho_v}\zeta\right)\right)\right] \tag{24}$$

where $f(\zeta) = -\zeta \ln(1 - 1/\zeta)$. The problem then reduces to one of finding the properties of the function $f(\zeta)$, which has been sketched in Fig. 2. As seen in the figure, $f(\zeta)$ is a monotonically decreasing function for ζ in the range of 1 up to $+\infty$. The function becomes infinite as ζ approaches 1 from the right and tends asymptotically to $f(\zeta) = 1$ when the argument ζ becomes large. Since ρ_l/ρ_v will always be ≥ 1, it follows from the decreasing behavior of the function that $f(\zeta)$ must be greater that $f((\rho_l/\rho_v)\zeta)$. Therefore the net contribution of the compressibility terms to the right side of the constant-volume nucleation solution in equation (24) will be negative.

Several other qualitative conclusions about homogeneous nucleation at constant volume are also evident from equation (24). First of all as $V \to \infty$, ζ will tend to infinity so that both $f(\zeta)$ and $f((\rho_l/\rho_v)\zeta)$ approach 1. Hence for a large container, the compression terms in equation (24) will cancel one another and reduce the new constant-volume result for r_c to the familiar constant-pressure solution from equation (20), with the nucleation frequency J still given by equation (22). Such behavior makes sense physically because for large volumes the new vapor bubble is small relative to V, and only slight compression of the surrounding liquid takes place because of the constant-volume boundary condition. Then the system's options for storing excess availability would be essentially the same as in the constant-pressure case. Another observation from equation (24) is that the liquid compression terms would identically cancel to return the isobaric result if $\rho_l = \rho_v$, since a vapor bubble would then occupy the same volume as the liquid from which it was formed. Thus no additional pressure could be exerted on the surrounding liquid. This fact means that the impact of the compression terms on nucleation will vanish as initial conditions approach the critical point.

One of the best ways to visualize the solution characteristics is to examine $\partial^2 \Delta A/\partial r^2$ calculated from equation (18), which describes the overall shape of the system's excess availability curve as a function of bubble radius. The resulting expression for $\partial^2 \Delta A_V(r, V)/\partial r^2|_{r=r_c}$ is:

$$\left.\frac{\partial^2 \Delta A_V(r, V)}{\partial r^2}\right|_{r=r_c} = -8\pi\sigma + \frac{12\pi r_c}{\kappa_t}\left[\frac{1}{\zeta - 1} - \frac{1}{(\rho_l/\rho_v)\zeta - 1}\right] \tag{25}$$

where $\zeta = V/\frac{4}{3}\pi r_c^3$ as before. Except very close to the critical point $\rho_l \gg \rho_v$, and it is possible to neglect the second term inside the brackets relative to the first. Hence it follows that

$$\left.\frac{\partial^2 \Delta A_V(r, V)}{\partial r^2}\right|_{r=r_c} < 0 \quad \text{if} \quad r_c < \tfrac{2}{3}\sigma\kappa_t(\zeta - 1)$$

and

$$\left.\frac{\partial^2 \Delta A_V(r, V)}{\partial r^2}\right|_{r=r_c} > 0 \quad \text{if} \quad r_c > \tfrac{2}{3}\sigma\kappa_t(\zeta - 1). \tag{26}$$

Since r_c gives the values of r for which $\partial \Delta A_V/\partial r = 0$, one would expect the smaller r_c solution to correspond to a local maximum in the excess availability curve and the larger r_c value to be a local minimum. The initial local maximum in $\Delta A_V(r, V)$ constitutes the potential energy barrier to homogeneous nucleation as seen in the constant-pressure solution, while the local minimum indicates there will be an ultimate limit on bubble growth in a constant-volume environment. From both continuity of the thermodynamic potential curve and the physics of the problem itself, no more than these two critical points can be present, and under certain circumstances there may be only one or none at all.

Another question that needs to be answered is how the maximum and minimum of the availability curve behave as functions of V. Thus one must examine the derivative $\partial r_c/\partial V$ obtained by implicit differentiation of equation (23), which yields:

$$\frac{\partial r_c}{\partial V}(4\pi r_c^2)\left[\frac{2\sigma}{3r_c} + \frac{1}{\kappa_t}\xi\right] = \frac{kT_l}{V} + \frac{1}{\kappa_t}\left[\frac{\rho_l}{\rho_v}\ln\left(1 - \frac{4\pi r_c^3(\rho_v/\rho_l)}{3V}\right) - \ln\left(1 - \frac{4\pi r_c^3}{3V}\right) + \frac{4\pi r_c^3}{3V}\xi\right] \tag{27}$$

where

$$\zeta = \left[\left(1 - \frac{4\pi r_c^3(\rho_v/\rho_l)}{3V}\right)^{-1} - \left(1 - \frac{4\pi r_c^3}{3V}\right)^{-1}\right]$$

has been defined to make the notation more compact. Equation (27) can be rewritten by introducing the parameter ζ and expanding the logarithmic terms on the right side in a power series. Higher order terms are then neglected and the assumption $\rho_l \gg \rho_v$ is invoked to show

$$\frac{\partial r_c}{\partial V}(\text{at the local max.}) > 0 \quad \text{if} \quad \left[\frac{kT_l}{V} - \frac{1}{2\zeta^2\kappa_t}\right] > 0$$

$$\frac{\partial r_c}{\partial V}(\text{at the local min.}) < 0 \quad \text{if} \quad \left[\frac{kT_l}{V} - \frac{1}{2\zeta^2\kappa_t}\right] > 0. \tag{28}$$

If the group of terms inside the brackets is <0, the sign of $\partial r_c/\partial V$ for both critical points will be reversed. The kT_l/V term inside the bracket arises because of alterations in the nucleation frequency calculated from equation (22) when the container volume changes. On the other hand, the second quantity determining the sign of $\partial r_c/\partial V$ is due to the influence of V on r_c through the logarithmic compression terms in equation (23).

The qualitative variation in the r_c solutions can now be readily deduced from these derivative relations. The primary results that must be derived are the behavior of the smaller r_c root, which corresponds to the local availability maximum, over the entire range of V and how the larger r_c solution changes relative to the smaller one as the container volume is reduced. When the container volume is large, the inequalities in equation (28) will be satisfied so that $\partial r_c/\partial V$ (at the local maximum) is positive. Thus the r_c value of the availability maximum will shift toward smaller bubble radii as V is reduced from ∞ to values where the compression terms become significant. For V sufficiently small, the second quantity inside the brackets in equation (28) will eventually overtake the nucleation frequency term. In this regime, reducing V causes the maximum of the excess availability curve to shift toward bigger r values while the larger r_c root declines. Thus the two r_c solutions of the homogeneous nucleation expression from equation (23) converge to meet each other as container volume decreases. When one reaches the situation where

$$r_c|_{\text{infl}} = \tfrac{2}{3}\sigma\kappa_t(\zeta - 1) \tag{29}$$

the local maximum and minimum of the potential curve will unite to form a single inflection point. Any smaller container volume has no r_c value associated with it, and homogeneous bubble nucleation cannot take place under such conditions.

Tracking the larger r_c solution from the basic constant-volume homogeneous nucleation relation given by equation (23) is vital to understand the overall shape of the availability curve and locate the container volume for the inflection point. However the larger r_c root of equation (23) does *not* itself represent the greatest size a bubble can attain at that particular container volume. The smaller and larger solutions from equation (23) are the critical radii that would align the energy level for the J from equation (22) with the maximum and minimum of $\Delta A_v(r, V)$, respectively. Since the height of the potential hill formed by the maximum is the barrier that must be overcome for nucleation, the smaller r_c from equation (23) is the appropriate one to use in calculating the depressurization necessary for homogeneous nucleation at constant volume. The larger r_c value from equation (23) with $r_c > \frac{2}{3}\sigma\kappa_t(\zeta - 1)$ places the local *minimum* in $\Delta A_v(r, V)$ at the energy level of the specified J, which has no physical basis. Except as a guide to the behavior of the smaller r_c value when it approaches the inflection point, the larger root is extraneous.

The actual upper limit of bubble growth, r_{max}, for a given container size is calculated by returning to equation (18) and setting $\partial \Delta A_v(r, V)/\partial r = 0$ with r_c equal to the smaller solution from equation (23). Carrying out the differentiation and rearranging slightly yields:

$$\left.\frac{\partial \Delta A_v(r, V)}{\partial r}\right|_{r = r_{max}} = 8\pi\sigma\left(r_{max} - \frac{r_{max}^2}{r_c}\right)$$

$$+ \frac{4\pi r_{max}^2}{\kappa_t}\left[\ln\left(1 - \frac{4\pi r_{max}^3}{3V}\frac{\rho_v}{\rho_l}\right) - \ln\left(1 - \frac{4\pi r_c^3}{3V}\frac{\rho_v}{\rho_l}\right)\right.$$

$$\left. + \ln\left(1 - \frac{4\pi r_c^3}{3V}\right) - \ln\left(1 - \frac{4\pi r_{max}^3}{3V}\right)\right] = 0. \tag{30}$$

Since r_c is a trivial solution to this equation, it is necessary to solve for $r_{max} > r_c$ (small solution). As the specified chamber volume becomes smaller, the maximum bubble radius calculated from equation (30) will also decline until $r_{max} = r_c$, where r_c represents a single inflection point as described by equation (29). Under these conditions homogeneous nucleation is possible, but the bubble cannot grow further once formed. If the depressurization driving nucleation is accompanied by freezing of liquid inside the chamber, the calculated r_{max} would gradually increase as solid formed and the bubble accommodated the solidification shrinkage.

One final qualitative characteristic of the excess availability curves at constant volume deserves mention. The constant-volume nucleation solution in equation (23) can be interpreted as

$$kT_l \ln\left(\frac{N_{av}\rho_l kT_l V\tau}{Mh_p}\right) = \Delta A_v(r_c, V) \tag{31}$$

so it is possible to calculate how the energy level of the local availability maximum behaves as a function of container volume. Taking the derivative with respect to V gives:

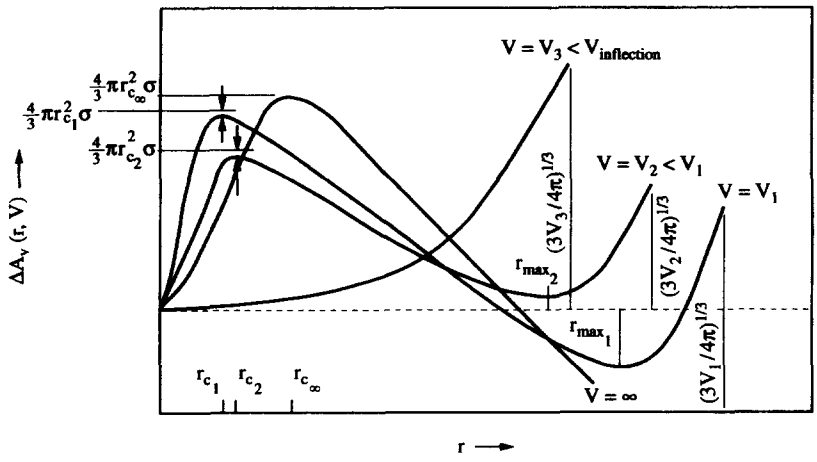

Fig. 3. Excess availability potential curves under constant volume conditions for various container sizes.

$$\frac{d\Delta A_V(r_c, V)}{dV} = \frac{kT_l}{V} > 0. \quad (32)$$

Hence the relationship between $\Delta A_V(r_c, V)$ and V is a direct one. As the container size is reduced, the peak of the availability curve will shift downward at an increasing rate. Apparently $|\Delta A_V(r_c, V)| \leq \frac{4}{3}\pi r_c^2\sigma$ where r_c is the smaller solution for the local maximum, with equality only in the case of $V \to \infty$. For any finite container volume, there will be some deduction from the peak availability value $\frac{4}{3}\pi r_c^2\sigma$ expected from constant-pressure theory, due to the net negative contribution of the logarithmic liquid-compression terms on the right side of equation (23).

Most of the preceding discussion in this section can be effectively summarized by constructing a plot of $\Delta A_V(r, V)$ vs r for several values of V, as shown in Fig. 3. This graph illustrates the constant-volume counterpart of the familiar constant-pressure curve from Fig. 1, and excess availability potential curves for four different container volumes are given on the figure. In order to show clearly how the curves shift as V changes, Fig. 3 is not drawn to scale. For an infinitely large container volume, the potential curve in Fig. 3 displays a single peak and then slopes down to the right for all larger r, as seen in constant-pressure nucleation. Specifying V equal to some finite volume V_1 causes the local maximum to shift downward to a lower energy level and also move left to a new critical radius r_{c1} due to the influence of the new volume on the nucleation frequency. At the same time, the availability curve for $V = V_1$ now displays a local minimum at $r = r_{max1}$ before turning upward again and terminating when r approaches $(3V_1/4\pi)^{1/3}$, the maximum bubble size that would fit inside the container.

A further reduction in container volume to $V_2 < V_1$ would again lower the energy level of the local maximum in the curve and increase the availability of the local minimum, which would now occur at $r_{max2} < r_{max1}$. The gap between the availability peak and $\frac{4}{3}\pi r_c^2\sigma$ also becomes larger as V decreases and the logarithmic terms in equation (23) become more significant. If V_2 was small enough that the logarithmic compression terms could no longer be neglected, r_{c2} would lie slightly to the right of r_{c1} on the new flatter availability curve. When V equals some volume V_3 smaller than the container size where $r_c = r_{max}$, the potential curve slopes upward for all bubble radii that will fit inside the container, as shown by the fourth plot in Fig. 3. Now formation of any bubble would be associated with increasing excess availability and homogeneous nucleation cannot take place.

Depressurization requirements for nucleation

Figure 4, which has been adapted from Lienhard *et al.* [13], illustrates the thermodynamic states associated with homogeneous vapor nucleation on a P–v diagram, with the scales somewhat distorted for clarity. Starting with saturated liquid at pressure P_o, there are basically two ways to superheat the liquid in order

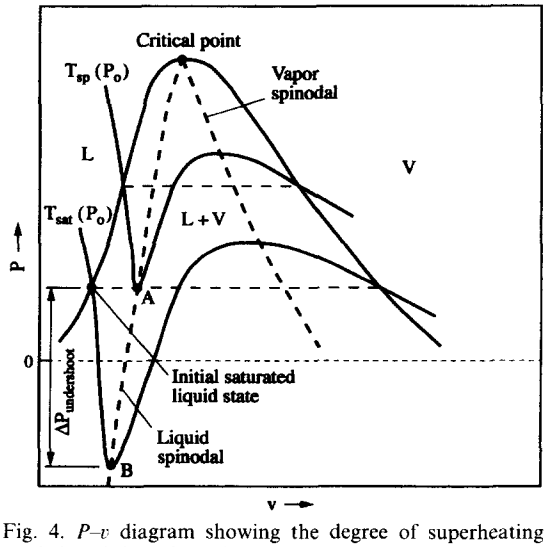

Fig. 4. P–v diagram showing the degree of superheating needed to bring about homogeneous nucleation by either temperature increase or depressurization.

to bring about homogeneous nucleation. On the P–v diagram, the $T = T_{sat}(P_o)$ isotherm represents the locus of all points at the initial temperature, and similar-shaped curves exist for other liquid temperatures. The liquid spinodal line linking the minimum of each temperature isotherm shows the absolute limit of metastable superheated liquid behavior that indicates homogeneous vapor formation. One way to achieve homogeneous nucleation is to increase the liquid temperature to T_{sp} while holding the pressure constant at P_o, so that the liquid strikes the spinodal line at point A. The other technique involves depressurizing the system at constant temperature $T_{sat}(P_o)$, so that point B is reached on the spinodal line. Now the driving force for nucleation is the pressure undershoot ΔP instead of the superheat temperature. It should be noted that the $\Delta P_{undershoot}$ necessary for nucleation may be larger than the initial absolute system pressure, causing point B to correspond to a negative absolute pressure as shown. Under these conditions, one must place the liquid in sufficient 'tension' to reach the spinodal in order to bring about homogeneous vapor formation. Although such negative absolute pressures are nonequilibrium phenomena that cannot persist over time, they can occur for brief intervals during the course of the nucleation process.

Homogeneous bubble nucleation during void formation while freezing a PCM is driven by depressurization as the phase change liquid shrinks upon cooling. Thus the ultimate objective is to calculate the total depressurization, ΔP_{tot}, required to nucleate. In the most general case, ΔP_{tot} will have two components.

$$\Delta P_\sigma = 2\sigma/r_c \tag{33}$$

is the amount of pressure drop required to satisfy Laplace's equation for mechanical equilibrium of the vapor bubble. This component of the required pressure undershoot will always be present. If the container volume is small enough that liquid compression effects are significant, there will be a second component of ΔP_{tot} given by

$$\Delta P_{comp} = \frac{1}{\kappa_t}\left\{\ln\left(1 - \frac{4\pi r^3}{3V}\left(\frac{\rho_v}{\rho_l}\right)\right) + \ln\left(1 - \frac{4\pi r^3}{3V}\right)\right\} \tag{34}$$

which is obtained from equation (15). The quantity ΔP_{comp} is the depressurization required to offset liquid compression resulting from appearance of a vapor bubble. One then calculates the total depressurization from

$$\Delta P_{tot} = \Delta P_\sigma + \Delta P_{comp}. \tag{35}$$

Numerical examples

To provide a numerical example of homogeneous nucleation calculations under constant-volume boundary conditions, solutions were obtained for homogeneous vapor formation in saturated liquid water at 25°C. These results are summarized in Tables 1 and 2 for container sizes ranging downward from $V = 1$ m^3. The necessary water properties were found in standard steam tables except for the liquid isothermal compressibility, which was taken from the results of Alamgir *et al.* [14]. Saturated liquid was chosen as the initial condition because the liquid must reach the saturation line on a P–v diagram before any bubbles can be nucleated. If the PCM liquid were initially compressed at a pressure above saturation, cooling would simply produce saturated liquid at a lower temperature and pressure prior to any nucleation. All the results in Tables 1 and 2 were calculated using $\tau = 1$ s in the homogeneous nucleation frequency. Of course, using a longer τ makes nucleation easier by providing more time for it to occur, while a shorter τ reduces the likelihood that a bubble can be formed. Since one is interested in the smallest depressurization that would bring about nucleation within a reasonable period of time, a fairly long τ is called for relative to molecular collision time scales. Changing τ to 10^{-6} s decreased the critical radii in Table 1 by up to 32.6% and reduced V_{infl} by a factor of 2.3, while using $\tau = 10^3$ s increased the critical radii up to 10.6% and raised V_{infl} to 1.48 times the value in the table. Thus the solution is not particularly sensitive to τ over a relatively broad range, and $\tau = 1$ second was chosen as a reasonable compromise when compiling the tables.

In Table 1, the true critical radius for each volume was obtained by numerically solving equation (23) for the smaller r_c root, while the second column shows the r_c that would be calculated when neglecting the compression terms. The maximum bubble growth radii were then figured using equation (30). Table 2 also shows the pressure drop components calculated from equations (33)–(35) for the corresponding critical radii with $T_l = 25$°C. Compressibility effects do not become important in the critical radius or pressure drop calculations until $V \approx 10^{-23}$ m^3, and they then play an increasingly vital role until $r_c = r_{max}$ is reached at $V_{infl} = 0.115 \times 10^{-24}$ m^3, where equation (29) is satisfied. For smaller container sizes, no r_c solution exists and nucleation is not possible at $T_l = 25$°C. One should note that r_c declines with V till the compressibility terms become significant and then increases slightly as it approaches the inflection point value. The maximum bubble radius r_{max} always gets smaller when container volume is reduced, while the total depressurization ΔP_{tot} necessary for homogeneous nucleation rises over the entire range of decreasing V. These trends reflect the greater difficulty of bubble formation and growth in a more restricted space.

Tables 3 and 4 contain the critical radii and pressure drop results for homogeneous nucleation starting from saturated liquid water at $T_l = 250$°C with various size containers. The general trends of r_c, r_{max} and ΔP_{tot} for different container volumes are similar to those observed with the $T_l = 25$°C solutions. However com-

Table 1. Critical and maximum bubble radii for $T_l = 25°C$

Container volume [m³]	Critical radius neglecting liquid compression effects [m]	True critical radius [m]	Maximum bubble growth radius [m]
1	1.1382×10^{-9}	1.1382×10^{-9}	2.3770×10^{-1}
10^{-9}	1.0066×10^{-9}	1.0066×10^{-9}	2.4733×10^{-4}
10^{-18}	8.5500×10^{-10}	8.5500×10^{-10}	2.6038×10^{-7}
10^{-23}	7.5780×10^{-10}	7.5933×10^{-10}	5.5700×10^{-9}
10^{-24}	7.3682×10^{-10}	7.4413×10^{-10}	2.4473×10^{-9}
0.3×10^{-24}	7.2561×10^{-10}	7.5154×10^{-10}	1.5200×10^{-9}
0.115×10^{-24}	7.1656×10^{-10}	8.763×10^{-10}	8.763×10^{-10}

Table 2. Pressure decreases necessary for nucleation with $T_l = 25°C$

Container volume [m³]	ΔP_σ [Pa]	ΔP_{comp} [Pa]	ΔP_{tot} [Pa]
1	1.2669×10^8	—	1.2669×10^8
10^{-9}	1.4325×10^8	—	1.4325×10^8
10^{-18}	1.6865×10^8	—	1.6865×10^8
10^{-23}	1.89904×10^8	4.01323×10^5	1.90305×10^8
10^{-24}	1.93783×10^8	3.77993×10^6	1.97563×10^8
0.3×10^{-24}	1.91873×10^8	1.30073×10^7	2.04880×10^8
0.115×10^{-24}	1.64556×10^8	5.43001×10^7	2.18856×10^8

Table 3. Critical and maximum bubble radii for $T_l = 250°C$

Container volume [m³]	Critical radius neglecting liquid compression effects [m]	True critical radius [m]	Maximum bubble growth radius [m]
1	2.5105×10^{-9}	2.5105×10^{-9}	1.9500×10^{-1}
10^{-9}	2.2214×10^{-9}	2.2214×10^{-9}	2.0297×10^{-4}
10^{-18}	1.8885×10^{-9}	1.8885×10^{-9}	2.1341×10^{-7}
10^{-22}	1.7200×10^{-9}	1.7241×10^{-9}	9.6124×10^{-9}
10^{-23}	1.6753×10^{-9}	1.7150×10^{-9}	4.0815×10^{-9}
0.4×10^{-23}	1.6571×10^{-9}	1.7798×10^{-9}	2.7205×10^{-9}
$0.2661787 \times 10^{-23}$	1.6490×10^{-9}	2.0173×10^{-9}	2.0174×10^{-9}

Table 4. Pressure decreases necessary for nucleation with $T_l = 250°C$

Container volume [m³]	ΔP_σ [Pa]	ΔP_{comp} [Pa]	ΔP_{tot} [Pa]
1	2.0793×10^7	—	2.0793×10^7
10^{-9}	2.3499×10^7	—	2.3499×10^7
10^{-18}	2.7641×10^7	—	2.7641×10^7
10^{-22}	3.02767×10^7	1.41436×10^5	3.04181×10^7
10^{-23}	3.04373×10^7	1.39344×10^6	3.18307×10^7
0.4×10^{-23}	2.93291×10^7	3.90118×10^6	3.32303×10^7
$0.2661787 \times 10^{-23}$	2.58762×10^7	8.56750×10^6	3.44437×10^7

Table 5. Initial liquid conditions such that $\Delta P_{tot} = P_{sat}(T_l)$

Container volume [m³]	Initial liquid temperature [°C]	Critical radius [m]	$\Delta P_{tot} = P_{sat}(T_l)$ [Pa]
1	298.55	3.4973×10^{-9}	8.407×10^{6}
10^{-6}	300.4	3.2937×10^{-9}	8.64×10^{6}
10^{-12}	302.8	3.0657×10^{-9}	8.94×10^{6}
10^{-18}	305.7	2.8087×10^{-9}	9.30×10^{6}
10^{-22}	308.2	2.6469×10^{-9}	9.63×10^{6}
0.5×10^{-22}	308.6	2.6651×10^{-9}	9.68×10^{6}
10^{-23}	No solution is possible		

pressibility effects began influencing the critical radius calculation for the larger volume of $V \approx 10^{-22}$ m³ at 250°C. The V value corresponding to an inflection point of the availability potential curve was $V_{infl} = 0.2661787 \times 10^{-23}$ m³ when $T_l = 250$°C. These results were also obtained using $\tau = 1$ s to provide a time scale for nucleation. As occurred with $T_l = 25$°C, the solution proved relatively insensitive to the choice of τ.

Given the decrease in the departure from equilibrium necessary for homogeneous nucleation when initial conditions near the critical point, one would expect that for each V there would exist some initial liquid temperature such that $\Delta P_{tot} = P_{sat}(T_l) = P_o$. Hence the initial liquid saturation pressure would be just sufficient to provide the pressure drop needed for nucleation without placing the liquid in tension. Table 5 records the initial liquid temperatures necessary to have $\Delta P_{tot} = P_{sat}(T_l)$ for container volumes ranging from 1 m³ down to 0.5×10^{-22} m³. As expected, the T_l for equilibrium nucleation increases as V is reduced since the initial bubble will be harder to initiate in a smaller container. When $V \leqslant 10^{-23}$ m³ the critical radius bubble becomes comparable in size to the container volume, and it is no longer possible to find an equilibrium nucleation solution. Homogeneous nucleation must then take place by nonequilibrium depressurization that 'tears' the liquid to initiate a vapor bubble.

The preceding analysis should lead to increased understanding of the homogeneous nucleation process at constant volume and how it differs from the more classical constant pressure solutions already available. Like the earlier isobaric nucleation results, constant-volume homogeneous nucleation requires a substantial deviation from ordinary equilibrium states in order to take place. Achieving the necessary liquid superheats without first encountering heterogeneous nucleation is only possible under very closely controlled conditions which seldom occur naturally. It is hoped this experimental obstacle can eventually be overcome, allowing the new equations to be subjected to proper verification and providing further insight into the way vapor bubbles are nucleated in isochoric situations.

CONCLUSIONS

(1) For homogeneous nucleation at constant volume, there exist both an initial critical radius and a maximum ultimate bubble size due to compression of the remaining liquid.

(2) Increasing the container volume and raising the initial liquid temperature both decrease the necessary pressure undershoot for nucleation.

(3) There exists a particular container volume for any specified temperature below which homogeneous nucleation is impossible. Likewise, at most volumes there is a minimum liquid temperature for nucleation without placing the liquid in tension.

(4) The constant-volume nucleation equations reduce to their more familiar constant-pressure counterparts in the limiting case as the container volume becomes very large or initial liquid conditions approach the critical point.

(5) Like homogeneous nucleation under constant pressure, constant-volume nucleation can only occur under relatively specialized circumstances where heterogeneous nucleation is not a factor. It is unlikely to be observed in commonplace phenomena.

Acknowledgements—This material is based upon work partly supported under the first author's University of Kentucky Dissertation Year Fellowship, and additional funding was provided by the Air Force Aero Propulsion and Power Laboratory, Contract F33615-87-C-2777. The authors would also like to thank Dr. Chi-Sing Man for reviewing a partial draft of this manuscript and making many helpful suggestions.

REFERENCES

1. C. D. Sulfredge, L. C. Chow and K. A. Tagavi, Void formation in radial solidification of cylinders, *J. Solar Energy Engng* **114**, 32–39 (1992).
2. C. D. Sulfredge, L. C. Chow and K. A. Tagavi, Solidification void formation in tubes: role of liquid shrinkage and bubble nucleation, *Exp. Heat Transfer* **5**, 147–160 (1992).
3. C. D. Sulfredge, L. C. Chow and K. A. Tagavi, Void formation in unidirectional freezing from above, *Exp. Heat Transfer* **6**, 1–16 (1993).
4. A. W. Adamson, *Physical Chemistry of Surfaces* (4th Edn), pp. 6–9. John Wiley, New York (1982).
5. D. Turnbull, Formation of crystal nuclei in liquid metals, *J. Appl. Phys.* **21**, 1022–1028 (1950).

6. J. H. Holloman and D. Turnbull, Nucleation, *Prog. Metal Phys.* **4,** 333–388 (1953).
7. J. G. Collier, *Convective Boiling and Condensation*, pp. 113–115. McGraw-Hill, New York (1972).
8. B. Chalmers, *Principles of Solidification*, pp. 62–90. John Wiley, New York (1964).
9. V. P. Carey, *Liquid–Vapor Phase-Change Phenomena*, pp. 138–145. Hemisphere, Washington (1992).
10. F. F. Abraham, *Homogeneous Nucleation Theory, The Pretransition Theory of Vapor Condensation*, pp. 19–23. Academic Press, New York (1974).
11. R. Cole, Boiling nucleation. In *Advances in Heat Transfer*, Vol. 10 (Edited by J. P. Hartnett and T. F. Irvine), pp. 85–166. Academic Press, New York (1974).
12. H. B. Callen, *Thermodynamics*, pp. 54–55. Wiley, New York (1960).
13. J. H. Lienhard, N. Shamsundar and P. O. Biney, Spinodal lines and equations of state : a review, *Nucl. Engng Des.* **95,** 297–314 (1986).
14. Md. Alamgir, C. Y. Kan and J. H. Lienhard, An experimental study of the rapid depressurization of hot water, *J. Heat Transfer* **102,** 433–438 (1980).